

Journal of Stress Analysis

Vol. 8, No. 1, 2023-24, 1-18



ORIGINAL RESEARCH PAPER

Investigation of the Effect of Nano-Al₂O₃ Addition on the Tensile and Flexural Strengths and Hardness of Friction Stir Processed Polycarbonate

Ahmad Abdolabas Komaz^a, Maziar Mahdipour Jalilian^{a,*}, Mahdi Karami Khorramabadi^b

Article info

Article history: Received 02 February 2023 Received in revised form 22 April 2023 Accepted 09 June 2023

Keywords:
Friction Stir Processing (FSP)
Nanoparticles
Polycarbonate
Plunge depth
Translational speed

Abstract

In this paper, the effects of two factors named plunge depth and translational speed on tensile strength, flexural strength, and hardness of polycarbonate reinforced with Al₂O₃ nanoparticles by friction stir processing (FSP) was investigated. To study the effects of the mentioned variables, design of experiments (DOE) and statistical analysis were used. Each of the factors was considered at five levels. A total of 14 specimens were subjected to FSP. It was found that the effect of plunge depth on the values of tensile strength, flexural strength, and hardness of the FSP-ed samples was more than the translational speed. Increasing the plunge depth from 0 to 0.4mm caused a 52.3% decrease in tensile strength and a 42.6% decrease in flexural strength. In addition, it was found that increasing the plunge depth had a stronger effect on the tensile strength and caused a more severe decrease in it. According to the statistical analysis, the optimal plunge depth and translational speed to create the highest tensile strength and flexural strength is 0 mm and 42-46mm/min, respectively. The hardness of the processed sample was inversely proportional to the plunge depth and translational speed. By increasing the plunge depth from 0 to 0.4mm and increasing the translational speed from 30 to 90mm/min, the hardness of the processed zone decreased by 38.8% and 32.6%, respectively.

Nomenclature

DOE	Design of Experiments	FSP	Friction Stir Processing
FSW	Friction Stir Welding	F	Amount of force in kilograms
UTS	Ultimate Tensile Strength	$\parallel \theta$	Angle of the pyramid
SEM	Scanning Electron Microscope	RSM	Response Surface Methodology
d	Average length of the diameter in mil-		
	limeters		

E-mail address: maziar.1986.2000@gmail.com doi 10.22084/JRSTAN.2024.28243.1248

ISSN: 2588-2597



^a Department of Mechanical Engineering, Kermanshah Branch, Islamic Azad University, Kermanshah, Iran.

^b Department of Mechanical Engineering, Khorramabad Branch, Islamic Azad University, Khorramabad, Iran.

^{*}Corresponding author: M. Mahdipour Jalilian (Assistant Professor)

1. Introduction

Friction Stir Processing (FSP) is a concept of Friction Stir Welding (FSW). The unique features of FSW can be used to develop new processes [1]. FSP can be used as a general process to modify the microstructure and change the composition at the desired positions. In such cases, FSP is a pure solid process technique which has unique capabilities such as superplasticity, casting correction, corrosion resistance, surface composite production, and microstructure homogenization. FSP involves the complex motion of a material and plastic deformation. The geometry of the tools and parameters within the process have a significant effect on the material flow pattern and temperature distribution and, consequently, on the microstructural changes of the material [1]. In recent years, several surface modification techniques such as laser energy melting operations, high-energy electron spectrum irradiation, plasma spraying, and sinter casting have been developed for surface modification. One of the processes that can affect the workpiece surface to a certain depth and produce nanocomposites is FSP. Due to the increasing use of polycarbonate in various industries because of their lightness and chemical resistance, the need to strengthen these materials because of their low strength has been felt more. Modification of polycarbonate is done by adding additives to it. Polymer composites are mixtures of polymers with organic and inorganic additives. In fact, these additives have certain geometries such as fibers, plates, and particles. When fibers, small plates, or particles are dispersed in the nanometer range, the resulting composites are known as nanocomposites. Nanocomposites have attracted the attention of many industries in recent years, including automotive, shipbuilding and aerospace, due to their suitable mechanical, electrical and thermal properties compared to conventional polymers, metals, and ceramics. Due to the importance of the mentioned factors, in the present study, the effect of Al₂O₃ nanoparticles on tensile strength and flexural strength of polycarbonate specimens processed by the FSP technique was investigated, and the effect of two factors named plunge depth and translational speed on tensile strength, flexural, strength and hardness of processed specimens were investigated as well. In following, some studies in this regard have been reviewed. Bozkurt et al. applied FSP on polyethylene at tool rotation speeds of between 1500 and 3000rpm and tool translational speeds between 45 and 115mm/min with a shoulder diameter of 18mm and a pin diameter of 6mm [2]. They measured temperature changes during the process between 120 and 165°C, while the polymer has a melting point of 132°C. The hole and crack observed in the root of the welded sample reduced the tensile properties of the weld. The effect of the critical parameters of FSP for polyethylene was also investigated by Saeedi and Givi which include the rotation speed and the translational speed within the range of 1000 to 1800rpm and 12 to 20mm/min, respectively [3]. The optimum weld strength of 75% of the base material strength was obtained only for an optimal combination of welding parameters. These results show the important effect of process parameters on welding results. Using analysis of variance, Rezgui et al. optimized the parameters of FSP for welding heavy polyethylene sheets to each other [4]. Arici and Selale [5] as well as Arici and Sinmazçelýk [6] welded polyethylene using conventional the FSW tools. To avoid defects in the root cracks of the weld, they performed two butt welding passes and used a rotational speed of up to 1000rpm and a translational speed of up to 60mm/min. They reported insufficient heat production for rotational speeds of 600 to 800rpm and suitable conditions for rotational speeds of 1000rpm. The authors also observed that, depending on the temperature, some of the material was removed from the weld during welding. Xie and Geng in a study investigated the microstructures created by FSP [7]. They observed that as the rotational speed decreased, the grain size in the stirred region decreased due to the reduction of the input heat. Akramifard et al. showed in their research that the use of FSP in producing the surface composite of copper reinforced with silicon carbide particles leads to an increase in microhardness up to twice that of the base metal [8]. Barmouz et al. observed in their research that the FSP in silicon carbide-reinforced specimens has a small elongation and that the tensile test results for both specimens with and without reinforcement show a decrease in yield strength [9]. Using FSP, Mishra et al. developed the Al-Sic composite layer on AA5083 aluminum and obtained a uniform distribution of Sic particles on the aluminum surface, showing the adhesion of the composite layer to the substrate in this case [10]. In this experiment, the rotational speed of the tool was considered 300rpm at two different values of translational speeds. Shafiei et al. developed an Al-Al₂O₃ surface nanocomposite layer on an aluminum alloy using FSP under a constant rotational speed of 1000rpm and a constant translational speed of 135mm/min, and they found that the presence of Al₂O₃ particles was also reduced and that the reduction in grain size, following the occurrence of dynamic recrystallization phenomenon, increased stiffness and consequently wear resistance [11]. In this research, the main factors of increasing the microhardness of the composite layer developed using FSP method were reported as a reduction in grain size and a more uniform particle distribution. Also, the improvement of the wear resistance of the composite layer is due to the increase in stiffness and the decrease in the average value of the friction coefficient. Qu et al. formed three-millimeter-thick composite layers, including alpha alumina and silicon carbide particles, on 6061 alu-

minum alloy [12]. The results obtained from hardness tests show a decrease in the hardness of processed aluminum compared to the primary aluminum due to the disappearance of the effect of precipitation hardening during processing; therefore, the researchers decided to expose formed composite layers with Al₂O₃ particles to solubilization heat treatment and precipitation hardening after the FSP operation to prevent the loss of the heat treatment effect and reduce the hardness of the welded samples. Devaraju et al. developed a composite layer including silicon carbide and graphite on 6061 aluminum alloy using FSP and studied the effect of the volume percentage of reinforcing particles and the rotational speed of the tool on the wear and mechanical properties of welded specimen [13]. It was found that tensile strength was lower than that of primary aluminum due to the brittleness of the matrix in all cases and also decreases with the increasing of rotational speed. Also, increasing the volume percentage of reinforcing particles from 4% to 8% has a negative effect on the yield strength. It has also been found that the formation of a composite layer consisting of separated silicon carbide and graphite particles between the composite pin and the steel disk increases the wear resistance of the composite and that the graphite particles act as a solid lubricant in this layer. Bahrami et al. investigated the effect of the geometric shape of the tool pin on the microstructure and mechanical properties of AA7075/SiC composite samples produced by FSP [14]. In this research, five types of pins with square, conical thread, triangular, four-groove square and four-groove cylindrical pins at a constant rotational speed of 125rpm and a constant translational speed of 40mm/min were used. The microscopic examination showed a more uniform distribution of ceramic particles using threaded pins, and agglomeration of particles with a four-groove cylindrical pin were reported to be more severe than the others. The particles aggregate as centers of stress concentration during loading and reduce stiffness.

2. Experimental Method

In this section, the specifications of the materials used in the tests, the devices used to perform the operations, and the tensile, flexural, and hardness tests are introduced. Also, how to perform the operations, how to prepare samples for tests and prepare images, and images of tools are presented. The final part of this section is dedicated to the introduction of the parameters studied in the research and design of experiments based on the response surface methodology.

2.1. FSP Tools

Hot work tool steels are used for applications with higher temperatures than normal ones [15]. Cold work

tool steels usually get ductile and their strength decreases when exposed to high temperature ranges [15]. High-speed steels do not soften at such temperatures, but their toughness and heat shock resistance are not suitable for use at high temperatures [15]. Hot work tool steels have relatively low carbon with maximum toughness and elements such as Mo, W, and Co are used to resist softening at high temperatures [15]. Adding vanadium to steel improves its thermal resistance [15]. Basically, vanadium is added to increase wear resistance [15]. Hot work tool steels are divided into two groups [15]. The main element of the first group is molybdenum and the main element of the second group is tungsten. Molybdenum steels usually show better toughness and thermal resistance than the tungsten group. This category is mostly used for hot work tool steels which are typically used to make hot forming tools for ferrous and non-ferrous allows at temperatures above 200°C [15]. Due to the fact that in FSP, very large thermal cycles are formed during the process, a tool must be used so that its function is maintained at high temperatures and its mechanical properties do not change. In the present study, H13 was used to make the tool. Table 1 shows the chemical composition of H13 [15].

In order to make the tool in the present research, H13 steel with a diameter of 20mm and a length of 25cm was prepared. After that, designing and preparing the dimensional drawings of the desired tool, a computer numerical control (CNC) milling machine was used for the reduction stage of the tool. By changing the geometric parameters of the tool, the material flow formed in the process changes significantly, and this change in the pattern and volume of the flow changes the mechanical quality of welded specimen.

The tool undergoes relatively large mechanical and thermal stresses in the welding process. Thermal hardening is typically used to extend the life of the tools used. In the present study, the tool is made under the thermal hardening cycle. To do this, the following steps were performed.

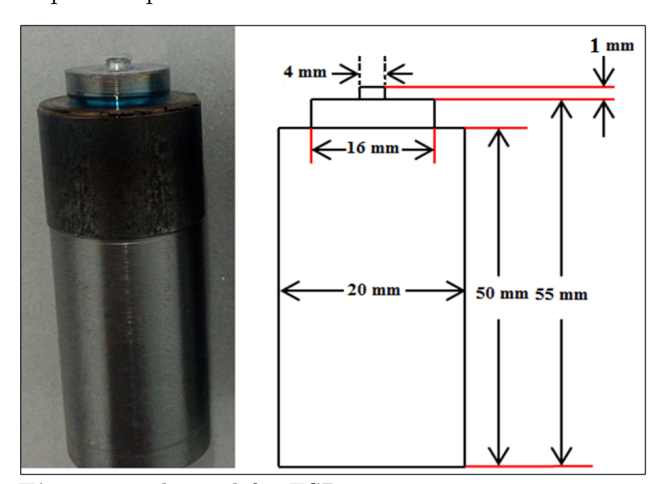


Fig. 1. Tools used for FSP.

Table 1 Percentage of chemical elements of H13 [15].

Chemical composition (wt%)									
Cr	Mo	Si	V	С	Ni	Cu	Mn	Р	S
4.75-5.5	1.1-1.75	0.8-1.2	0.8-1.2	0.32-0.45	0.3	0.25	0.2-0.5	0.03	0.03

- 1) Preheating stage: The preheating stage of the tools took place in two different steps. In the first step, the temperature of the tool increased with the rate of 222°C/h to reach 650°C. It should be noted that after reaching this temperature, the tool was kept at this temperature for an hour. In the second step, the temperature of the tools was increased to 850°C with the same rate as in the first step and it was kept at this temperature for an hour.
- Austinization stage: In this stage, the temperature rose immediately from 850 to 982°C, and the tools were kept at this temperature for 90 minutes.
- 3) Quenching stage: In this stage, a large tank of oil was prepared and the tools were taken out of the furnace and released in the tank. After cooling the tools to 450°C, they were taken out of the tank and the cooling process was continued in the open air until they reached room temperature.

2.2. Materials and Dimensions of Specimens

2.2.1. Polymer Used

Polycarbonate is the hardest transparent material used as a suitable alternative to glass in various parts of buildings. The structural diversity of polycarbonate sheets has made it possible to be easily used in any type of structures and near any type of building materials, and they have a wide range of applications. Table 2 shows the properties of polycarbonate used in the present study.

Table 2
Mechanical properties of the polycarbonate used.

Property	Value
Density [Kg/m ³]	1220
Ultimate Tensile Strength [MPa]	67
Elongation at fracture [%]	98
Shear Stress [MPa]	101
Flexural Strength [MPa]	80
Hardness (Vickers)	17

2.2.2. Cutting Parts

The purchased polycarbonate sheet was prepared in a thickness of 3mm. Components with dimensions of 120mm×120mm×3mm were used for all the FSP samples. An industrial guillotine was used to cut the parts.

2.2.3. Nanomaterials Used

 ${\rm Al_2O_3}$ nanoparticles were used to improve the mechanical properties of polycarbonate in the present study. For this purpose, nanoparticles with an average grain size of 20 to 30 nanometers were purchased from VCN Material. To perform FSP and add nanomaterials to the workpiece surface, grooves were made in the lower and upper surfaces of the workpiece. For each welding line, a groove was created in the upper surface and one groove in the lower surface with a depth of 1mm and a width of 0.5mm. These grooves were created with an industrial cutting machine. Fig. 2 shows some examples with the created grooves.

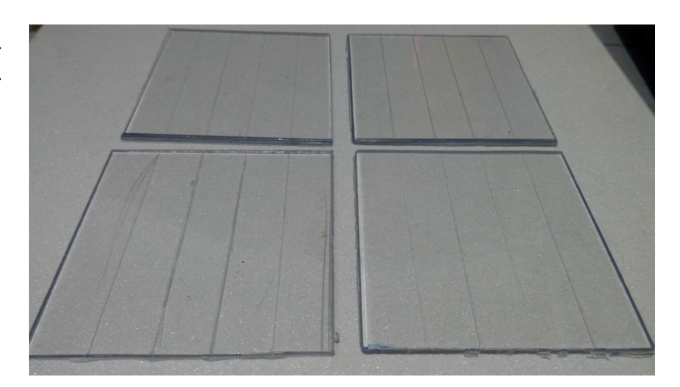


Fig. 2. Grooves created on the workpiece surfaces to embed nanoparticles.

2.3. Performing the Weld

2.3.1. Milling Machine

After cutting and preparing the parts, a milling machine was used to perform the parallel FSP. The most important features of this device are a powerful 11kW motor, a tool rotational speed up to 2000rpm, the ability to move the machine table in three directions, the complete control using the mechanical and adjustable equipment, the ability to set constant speeds in three directions, and the ability to set the device at the spindle angle. The column of the machine is made of cast iron in the form of a box, and the electric motor, drive mechanisms, gearbox, load mechanism, and the neck of the machine are mounted inside it. The neck of the machine is a steel axle in which the milling blades are fixed. The gearbox is designed to change the rotational speed of the neck (axis). The load gearbox is used to move the table in three directions. To perform the process, in the first stage, the bottom plate (anvil) and the appropriate fixture were prepared.

2.3.2. Welding Parameters

Due to the fact that the process parameters (translational speed and rotational speed of the tool) play an important role in the mechanical and microstructure properties of the welded parts, these parameters must be set in optimal condition. The two parameters of translational speed and plunge depth were considered as the studied variables. In the continuation of this section, the levels used for these two factors are presented. The rotational speed of the tool and the tilt angle of the tool were fixed for all samples and were considered 1180rpm and 2 degrees, respectively.

2.4. Mechanical Tests

2.4.1. Tensile Test

The engineering tensile test was used to show basic information about the strength of materials. To perform the tensile test, according to the standard, the SAN-TAM STM-250 (made in Iran) tensile test apparatus of Malayer University was used. Due to the fact that the surface conditions of the weld did not reach equilibrium because of the thermal cycles in the 2cm beginning and end of the welded zones, tensile test specimens needed to be prepared after separating these parts from the rest of the welded specimens. The dimensions of the samples were prepared according to ASTM-D638 standard [16]. Fig. 3 displays the dimensions of the tensile test specimen. It should be noted that two tensile test specimens were extracted from each welded specimen and the output results are based on the average results of the two specimens. All tensile tests were performed in the form of displacement control at a speed of 2mm/min.

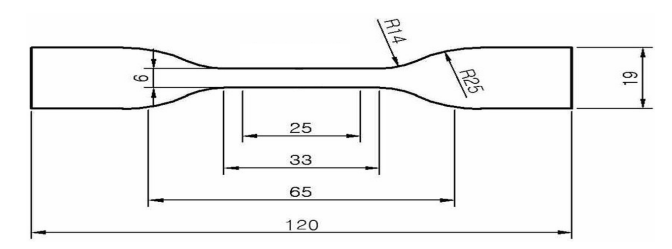


Fig. 3. Dimensions of tensile test specimens according to ASTM-D638 standard [16].

2.4.2. Three Point Bending Test

The three-point flexural test is a mechanical test that calculates the values of the modulus of flexural elasticity, flexural stress, flexural strain, and the stress-flexural strain response of a material. This test is performed by standard apparatuses, called universal testers, in a variety of geometries (such as three-point or four-point bending). In the present study, a three-point bending test was used to investigate the flexural

behavior of the welded specimens. This test is continued until a 90-degree angle is applied to the welding specimens. To perform this test, first, a three-point bending fixture was designed, and then bending tests were performed by the SANTAM STM-250 apparatus at Malayer University. The three-point bending test specimens in accordance with ASTME190-92 [17] is shown in Fig. 4. The flexural strength of the specimen under flexural testing is obtained by the following Eq. (1) [18]. In this equation, b, L, F, and d are the width of the beam, the length between the two rollers, the maximum applied force, and the thickness of the beam, respectively.

$$\sigma_f = \frac{3FL}{2bd^2} \tag{1}$$



Fig. 4. The three-point bending fixture used

2.4.3. Microhardness Test

Hardness is one of the inherent and fundamental properties of a substance. Hardness can be considered as the resistance of a material to plastic deformation, which includes permanent or localized deformation. There are various standards for performing this test. In this test, a descending pyramid with a square base is used. The angle of the faces in front of the pyramid is 136 degrees. Vickers hardness can be obtained using Eq. (2) [19].

$$HV = \frac{2F\sin\frac{\theta}{2}}{d^2} = \frac{1.854F}{d^2} \tag{2}$$

In this equation, F and d indicate force in kilograms and the average length of the diameter in millimeters, respectively. θ is the angle of the pyramid and is typically 136 degrees. In the present study, Vickers microhardness test was used to calculate the hardness of the processed samples. To perform the hardness test, five points were selected from the surface of the processed sample and their hardness was obtained. Finally, the mean hardness of the five points was reported as a result of the specimen hardness. The microhardness test of the samples was performed by a microhardness apparatus in 30 seconds under a load of 50 grams at room temperature.

2.5. SEM Images

Scanning electron microscope (SEM) is a type of electron microscope that can capture pictures of surfaces with a magnification of 10 to 500,000 times with a resolution of less than 1 to 20 nanometers. SEM is one of the most suitable apparatus available for testing and analyzing the morphology of nanostructures and identifying chemical compounds.

In the present study, SEM images were used to investigate the uniform distribution of nanoparticles in the sample section.

2.6. Design of Experiments (DOE)

The design and evaluation of experiments is a fundamental principle in the research of engineering science and technology. This will provide reliable data and reduce the time and number of tests. In experimental sciences and engineering researches, the decision making is based on experiments. The three basic principles in studies based on the statistical design are:

- Setting goals
- Design of experiments (DOE)
- Statistical evaluation

Response surface methodology (RSM) is a DOE method to improve product quality. The technique

used in this method includes how to design experiments and evaluate or analyze the results. This method studies the effect of factors on the response simultaneously and is one of the most important optimization methods by designing statistical experiments. RSM is a set of useful mathematical and statistical techniques for modeling and analyzing problems so that the optimal response, which is affected by several variables, is the optimal value of response. The relationship between the response and the factors x1, x2, ... and xk in RSM is $y = f(x_1, x_2, ..., x_k) + \varepsilon$, where ε indicates the error of the method. The function f in this relation is called the surface response. By obtaining the experimental data according to the desired design, the optimal value of the function y is calculated. In the present study, two main factors are considered as independent variables of the problem and three parameters are considered as the answer. Table 3 shows the variables studied in the research and their levels. Table 4 shows the design matrix.

3. Results and Discussion

To study the effect of the mentioned factors, DOE and statistical analysis by RSM were performed using Minitab software. Each of the presented factors was considered at five levels. A total of 14 specimens were subjected to FSP. This section presents the results and discusses it.

Table 3
Factors studied and their levels.

Factors	Unit	Level 1	Level 2	Level 3	Level 4	Level 5
translational speed	$\mathrm{mm/min}$	30	45	60	75	90
Plunge Depth	mm	0	0.1	0.2	0.3	0.4

Table 4
DOE table

Std order	Run order	Pt type	Blocks	Translational speed (mm/min)	Plunge depth (mm)
1	1	1	1	45	0.1
2	2	1	1	75	0.1
3	3	1	1	45	0.3
4	4	1	1	75	0.3
5	5	0	1	60	0.2
6	6	0	1	60	0.2
7	7	0	1	60	0.2
8	8	-1	2	30	0.2
9	9	-1	2	90	0.2
10	10	-1	2	60	0
11	11	-1	2	60	0.4
12	12	0	2	60	0.2
13	13	0	2	60	0.2
14	14	0	2	60	0.2

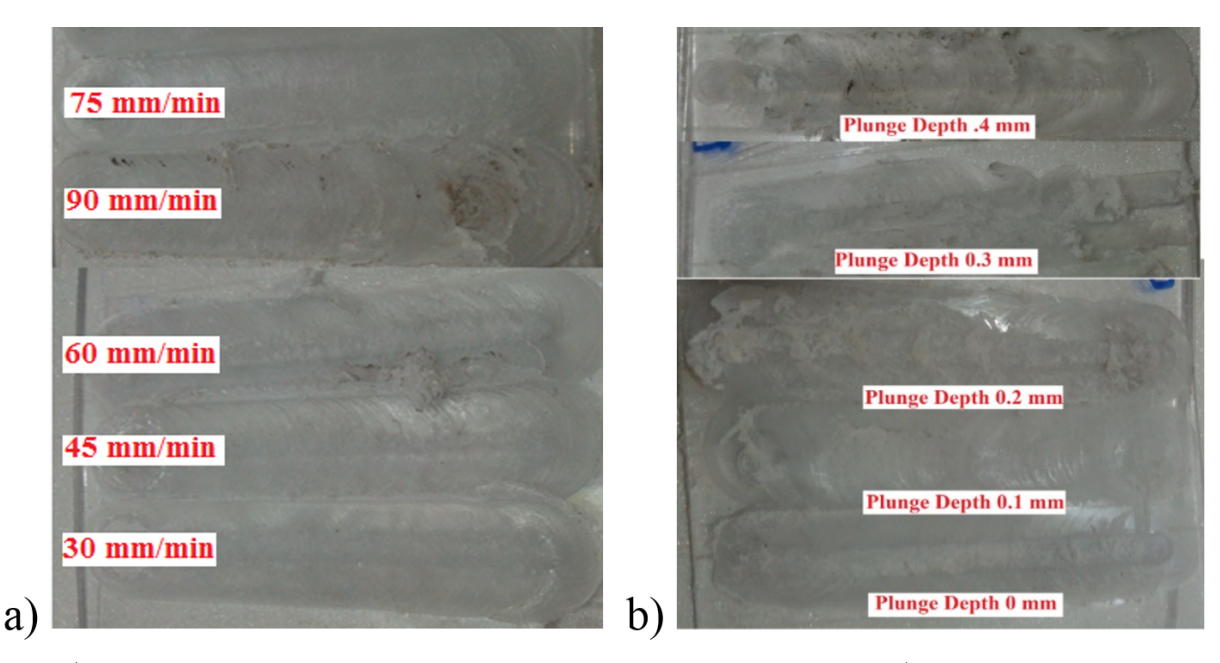


Fig. 5. a) Surface of processed samples with different tool translational speeds, b) The surface of the processed specimens with different plunge depths of the tool.

3.1. Macrography of Samples

3.1.1. Deliberation of the Upper Surface

In this section, first, the surface morphology of the processed samples is studied to discuss the effect of the two factors of translational speed and shoulder plunge depth on the surface quality of the processed area. Figs. 5a and 5b demonstrate the surface of the processed specimens with different translational speeds and different shoulder plunge depths, respectively.

As can be seen, the surface quality of the processed samples is strongly dependent on the two parameters of translational speed and plunge depth of the tool. As shown in Fig. 5a, at all tool translational speeds except 90mm/min, the sample surface is smooth and free of common defects such as cavities and protrusions. In the processed sample with a translational speed of 90mm/min, due to the high translational speed of the tool, the amount of heat accumulated in the processing area is reduced, eventually leading to cavities and relatively severe protrusions of the material in the upper region. In other processed specimen at other speeds, due to the stable plastic flow conditions, the processed surface is almost uniform and smooth. According to Fig. 5b, it was found that the tool shoulder plunge depth strongly affected the surface quality of the processed specimen. It can be seen that with increasing plunge depth, the surface quality decreased drastically and relatively large protrusions and cavities were created in the specimen surface. At two plunge depths of 0 and 0.1mm, the processed surface is relatively smooth and uniform and has a good quality, but at other plunge depths, the quality of the processed surface is not suitable, and protrusions and relatively large holes were created in the processed area (stirred zone). By comparing the two Figs. 5a and 5b, it was found that the plunge depth had a much stronger effect on the surface quality of the processed specimen than the tool's translational speed, and its change caused more drastic changes in the processing area.

3.1.2. Checking the Failure Section

Fractography is part of the science of metallurgy that is commonly used to identify the causes and manner of failure. In this method, the properties of the material are determined by using the fracture site and deliberating it by SEM and TEM microscopes. Fractography is a science that can determine how and in what direction bodies break through various computational and practical techniques. Various factors cause a body to break, such as bending, surface defects, or cracks. Also, fractography can provide the fracture stress and such information as the yield point and maximum tension. One area of concern in failure morphology is the fracture surface test. But in some cases, these experiments are not needed and only the size of the patterns and shapes that occur at the failure site are collected. In the present study, the failure section of tensile test specimens was investigated by changing the two parameters of translational speed and plunge depth. Fig. 6 illustrates examples of failure sections in processed specimens with different translational speeds.

With increasing the tool translational speed, the failure pattern of the processed specimen changes from ductile failure to brittle failure. Also, the fracture in the base material (pure polycarbonate) is completely smooth and uniform due to the uniform structure of this polymeric material.

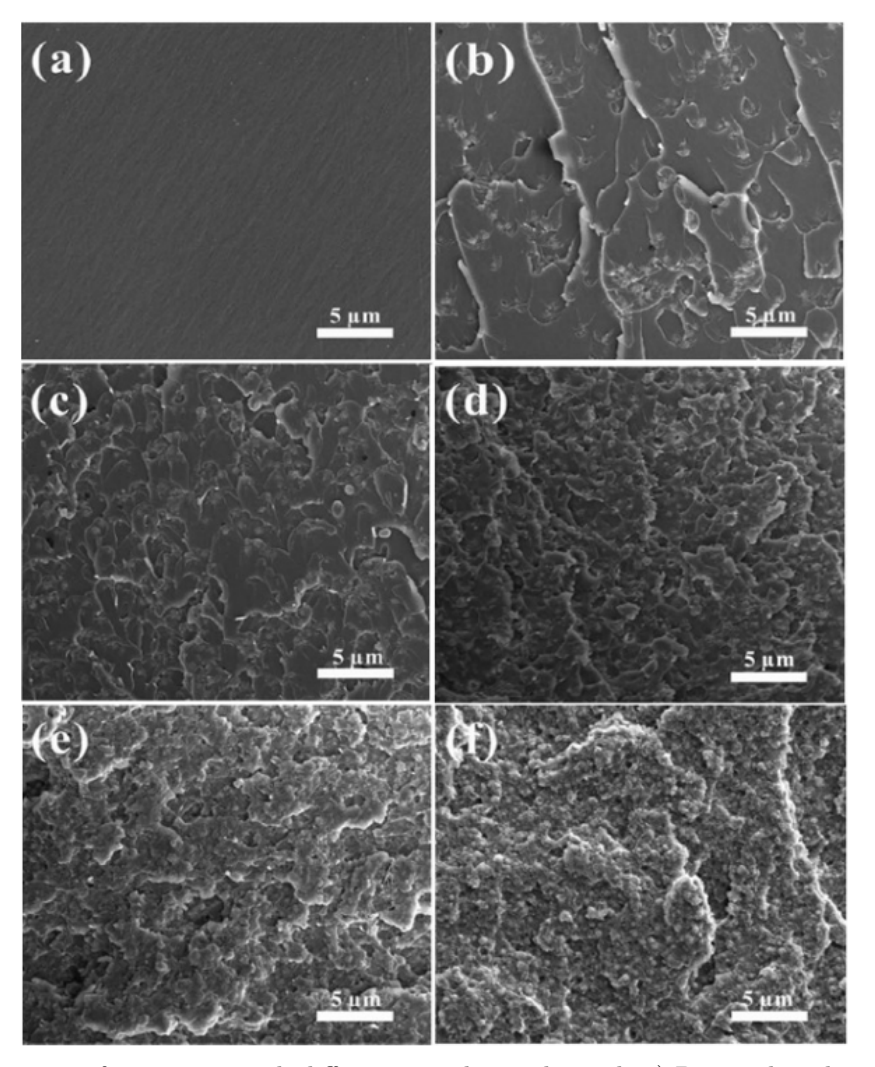


Fig. 6. Fracture section of specimens with different translational speeds a) Pure polycarbonate b) 30mm/min c) 45mm/min d) 60mm/min e) 75mm/min f) 90mm/min.

Pure polycarbonate has a fracture strain of approximately 100% [20]. It can be seen that in other samples, due to the addition of a secondary material (aluminum), the integrated structure of the processed sample has changed. In samples with aluminum nanoparticles, the distribution of these nanoparticles determines the type of failure of the specimen under loading. With increasing the translational speed up to 60mm/min, the cross-sectional failure is almost ductile, but at two translational speed of 75 and 90mm/min, the failure is quite brittle due to the accumulation of nanoparticles discontinuously in some areas. In order to investigate the effect of the plunge depth, the failure sections for the three plunge depths of 0, 0.2 and 0.4mm are shown in Fig. 7.

According to Fig. 7, increasing the shoulder plunge depth, as well as the translational speed, changes the type of cross-sectional failure from ductile to brittle. As can be seen in Fig. 7, increasing the plunge depth has caused severe discontinuities in the welding section. Changing the plunge depth changes the distribution of

nanoparticles and ultimately leads to a change in the failure pattern formed in the sample.

3.1.3. Investigation of Nanoparticle Distribution

Although the uniform distribution is very desirable, in most cases, it is not possible and the dispersion of nanoparticles is random. In the present study, dispersion was done and the placement of nanoparticles in polycarbonate was investigated. For this purpose, to investigate the effect of two parameters of translational speed and plunge depth on the distribution of Al_2O_3 nanoparticles in processed samples, the distribution of nanoparticles in the first, third, and fifth levels for the two factors is presented. Fig. 8 shows the distribution of nanoparticles in three processed samples with plunge depths of 0, 0.2, and 0.4mm. Fig. 8 also demonstrates the distribution of nanoparticles in three processed samples with translational speeds of 30, 60, and 90mm/min.

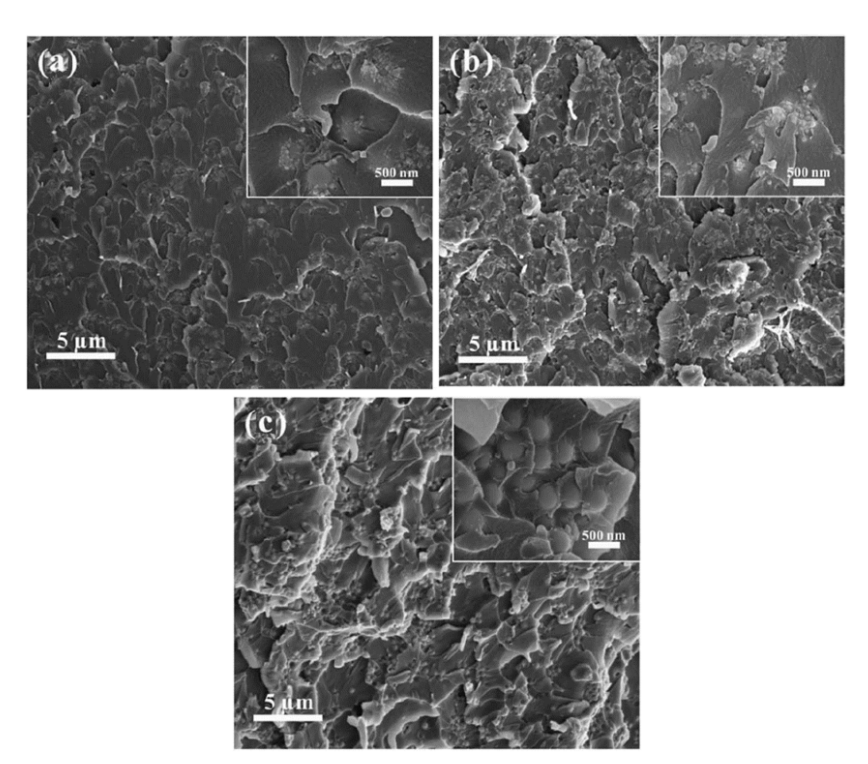


Fig. 7. Fracture section of specimens with different plunge depths a) 0mm b) 0.2mm c) 0.4mm.

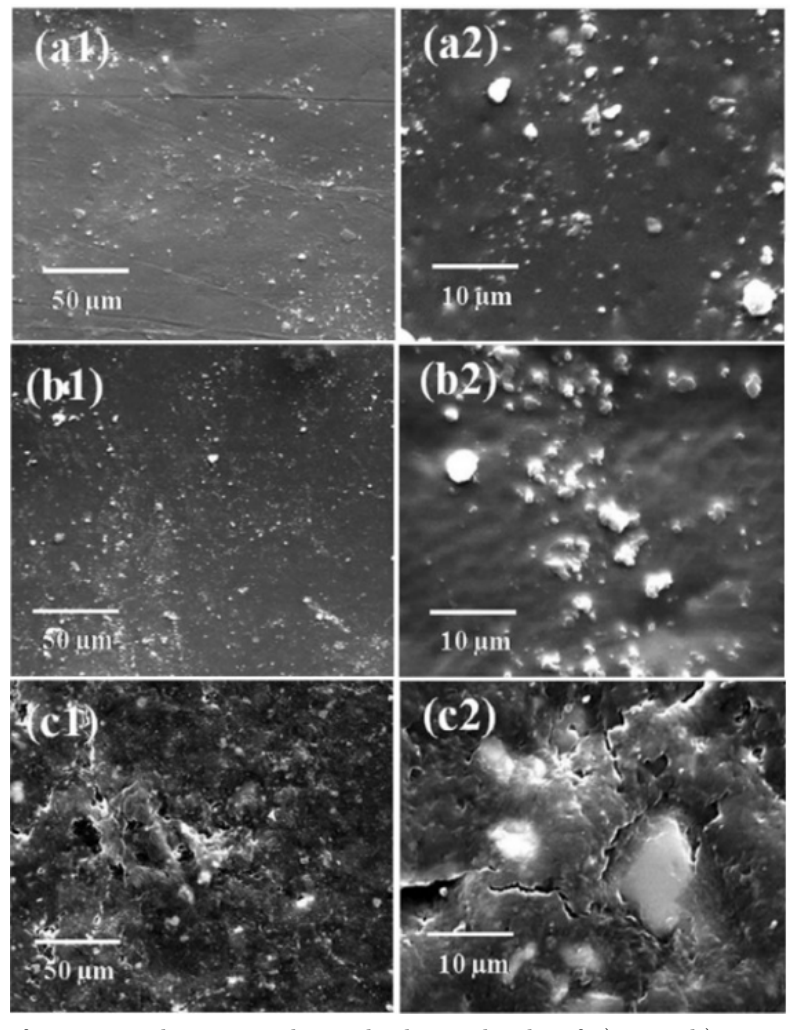


Fig. 8. Distribution of nanoparticles in samples with plunge depths of a) 0 mm b) 0.2 mm c) 0.4 mm.

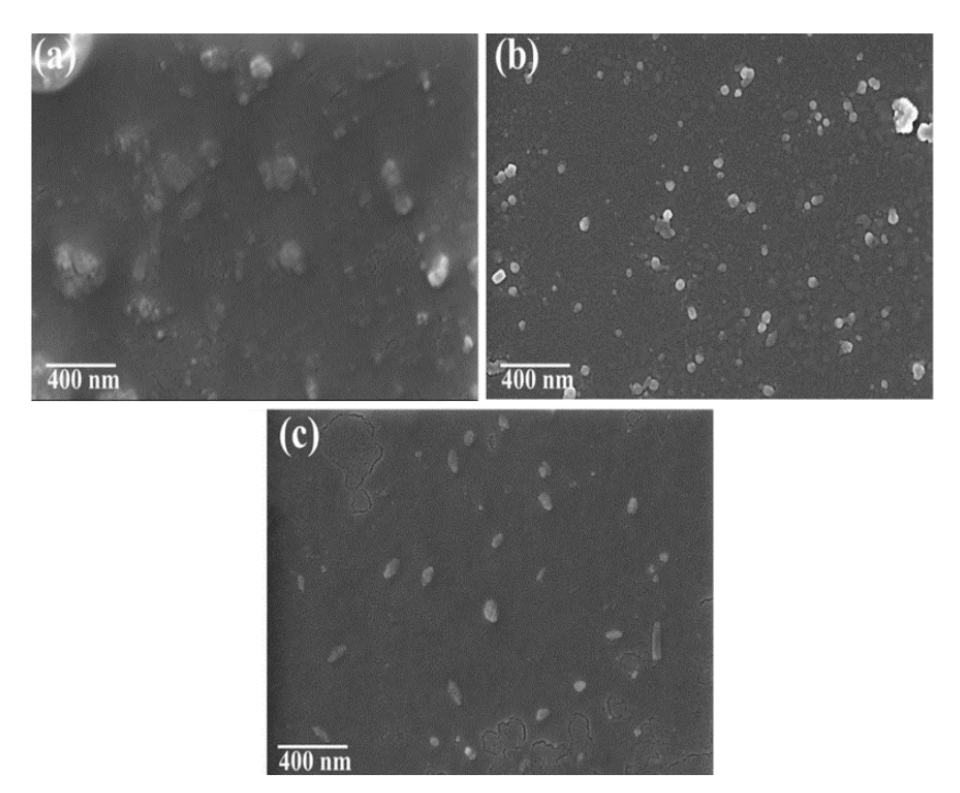


Fig. 9. Distribution of nanoparticles in samples with translational speeds of a) 30mm/min b) 60mm/min c) 90mm/min.

According to Figs. 8 and 9, a change in the plunge depth of the tool shoulder leads to a change in the pattern of distribution of nanoparticles in the polymer matrix. According to Fig. 7, it can be seen that with increasing the plunge depth of the tool in the processed area, the distribution quality of nanoparticles in the polymer matrix is drastically reduced. As can be seen, at a plunge depth of 0mm, the nanoparticles are distributed almost uniformly in the polymer matrix, and less agglomeration of nanoparticles is seen in the figure. However, in the images related to the two samples with plunge depths of 0.2 and 0.4mm, it can be seen that relatively severe agglomeration occurred in the processed section. As shown in Fig. 9, changes in the distribution of nanoparticles are evident in the processed samples with varying translational speeds. According to the figure, the particle distribution in the processed sample is formed almost uniformly at the translational speeds of 30 to 60mm/min. It should be noted that in the other two examples, the particle distribution is relatively uniform. Based on the images shown in Figs. 8 and 9, it was found that the translational speed has a far less effect on the nanoparticle distribution pattern than the plunge depth.

3.2. Results of Statistical Models

In this study, in order to comprehensively and appropriately investigate the effect of the factors on the answers of the problem, statistical design and analysis

was used. RSM based on the central composite design was used to design the experiment. Each factor was considered at five levels. Three variables tensile strength, flexural strength, and hardness were considered as output variables. The results are presented for each variable separately.

3.2.1. Tensile Strength

Table 5 shows the design table and the results of the tensile strength of the studied cases.

Table 5
Results of tensile strength of the studied cases

h	Results of tensile strength of the studied cases.								
	Run	Translational	Plunge depth	Ultimate tensile					
	${\rm order}$	${\rm speed}~({\rm mm/min})$	(mm)	strength (MPa)					
	1	45	0.1	89.4					
	2	75	0.1	72.5					
	3	45	0.3	72.3					
	4	75	0.3	62.1					
	5	60	0.2	71.6					
	6	60	0.2	73.1					
	7	60	0.2	70.9					
	8	30	0.2	70.7					
	9	90	0.2	63.8					
	10	60	0	94.3					
	11	60	0.4	61.9					
	12	60	0.2	74.1					
	13	60	0.2	72.3					
	14	60	0.2	73.5					

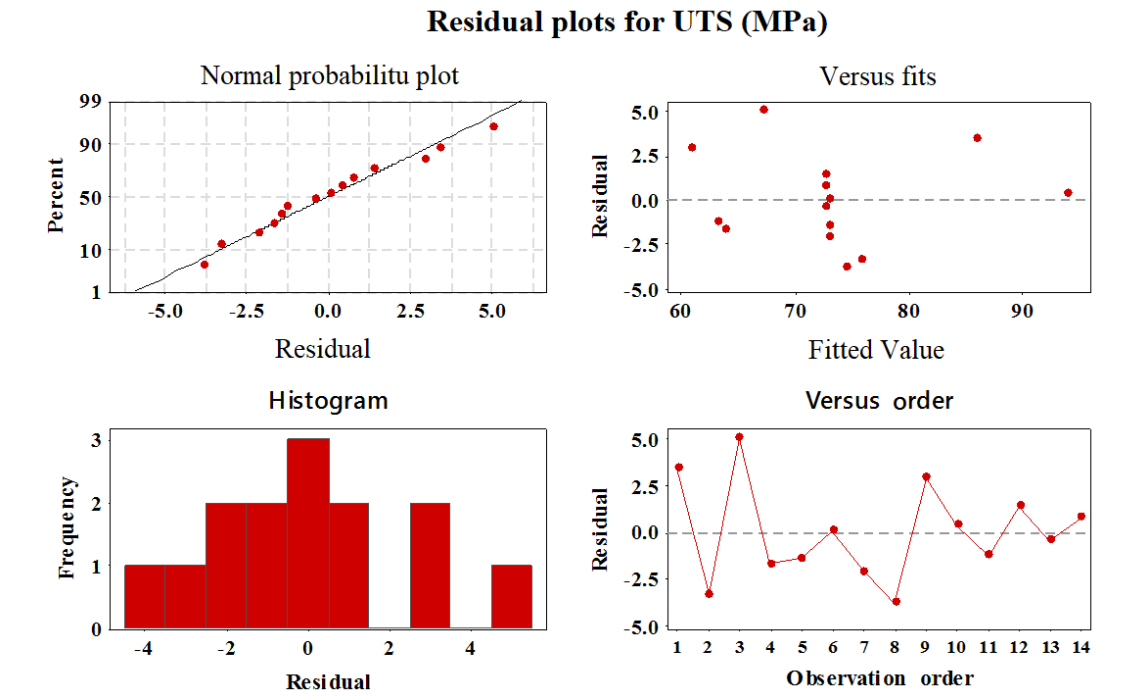


Fig. 10. Diagrams used to evaluate the adequacy of the statistical model of tensile strength.

The first step in statistical analysis using RSM is to use a statistical model with an appropriate degree. In the present study, a complete quadratic model was used for all models. In this model, the principal factors, the quadratic power of the principal factors, and the interactions of the factors were investigated. To evaluate the adequacy of the model, graphs of residual normality, constant variances, and independence of runs to time were used. These diagrams are displayed in Fig. 10.

Based on the Percent-Residual and Frequency-Residual diagrams, due to the lack of significant scattering of data (residues) from the normal line and the normal distribution of residual values, it was determined that the data were normally distributed and with these conditions, the data were assumed to be normal. Also, based on the diagram presented in the Residual-Fitted Value, and due to the lack of a special trend in the residuals compared to the fitted (predicted) values, the accuracy of the assumption that the variances were constant was determined, and according to the Residual-Observation Order diagram and the absence of a specific trend in residual values with respect to time and performing of experiments, the assumption that residual values were not time-dependent was proved. Based on the diagrams presented in Fig. 10, it was determined that the obtained data were sufficient. In other words, it can be said that this data was sufficient to investigate the effect of the factors on the tensile strength. The second step in the statistical study of a phenomenon is the need to identify the parameters affecting the response. Fig. 11 shows the Pareto chart of the effectiveness of the factors on the tensile strength of the processed specimens.

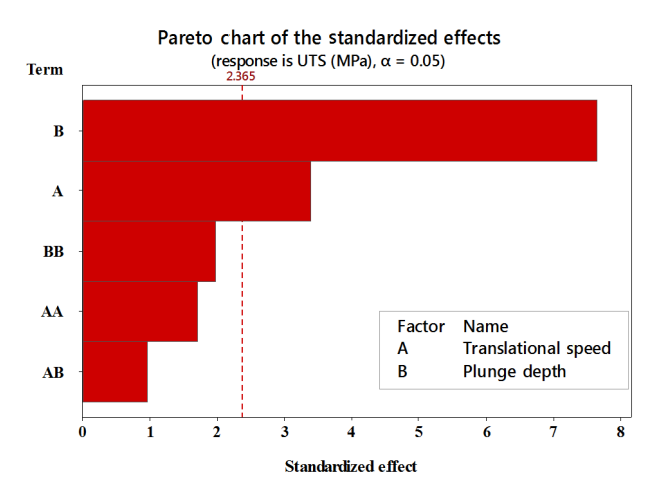


Fig. 11. Pareto chart to determine the order in which different factors affect tensile strength.

Due to the fact that the complete quadratic model was used, the parameters studied in the research include the main factors, the quadratic power of the main factors, and interactions. Based on the diagram presented in Fig. 11, it was found that the most effective parameters of the model on the tensile strength of the processed specimens was the tool's shoulder plunge depth and the tool's translational speed, respectively. According to Fig. 11, it was found that the other terms of the statistical model (interaction and quadratic factors) were ineffective. Figs. 12a and 12b display the effects of the main factors.

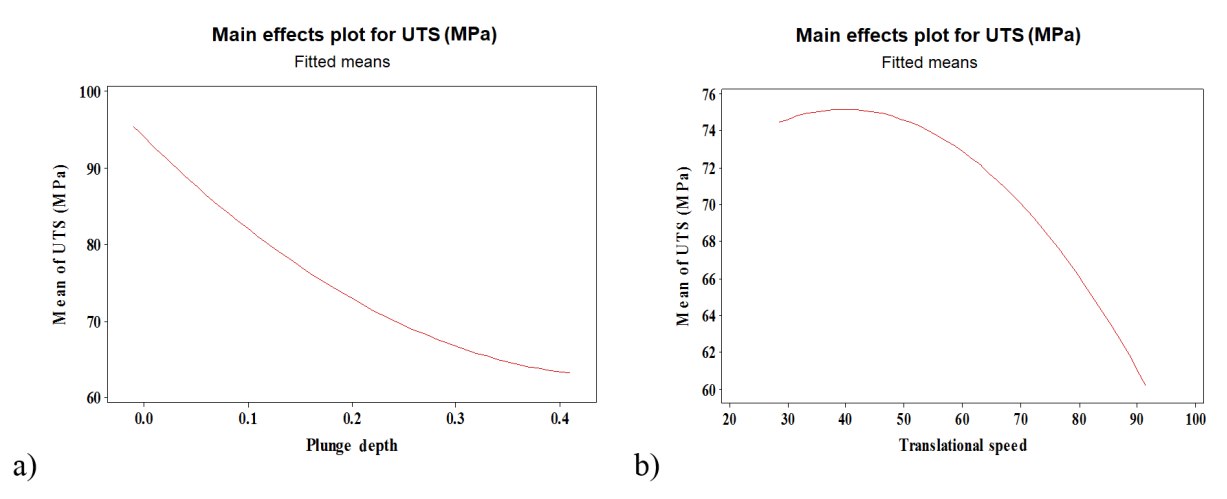


Fig. 12. a) Diagram of how the plunge depth affects the tensile strength, b) Diagram of how effective the translational speed is on the tensile strength.

Based on Fig. 12a, it was found that the plunge depth was inversely related to the tensile strength of the processed samples by FSP. According to Fig. 12a, with increasing the plunge depth, the tensile strength of the studied samples decreased sharply. Based on the statistical analysis, it was found that increasing the plunge depth from 0 to 0.4mm reduced the average tensile strength by 52.3%. Increasing the plunge depth of the tool has two consequences:

- Increasing the plunge depth causes an improper distribution of nanoparticles in the processed area, which causes a lack of promotion of mechanical properties in the section of the processed area and mechanical heterogeneity of the sample.
- Increasing the plunge depth reduces the thickness of the part, which reduces the stress concentration in the reduced areas and reduces the strength of the processed sample.

According to Fig. 12b, it was found that changing the tool's translational speed caused significant changes in the tensile strength of the processed samples. Translational speed changes can be deliberated in two different phases. In the first phase, increasing the translational speed from 30 to 45mm/min caused a relative increase in the tensile strength. But after increasing the translational speed of 45mm/min, the tensile strength decreased significantly with a slope. On average, the tensile strength of the processed specimens decreased by 20% as the translational speed increased from 45 to 90mm/min. It should be noted that the use of an appropriate and optimal translational speed leads to the formation of a proper plastic flow and a uniform distribution of nanoparticles in the cross section of the processed area, ultimately leading to the improved tensile strength of the sample. Eq. (3) shows the regression equation for statistical prediction of the tensile strength.

$$\label{eq:UTS (MPa) = 100.9 + 0.222 Translational Speed} \\ - 202.0 \ \text{Plunge Depth} \\ - 0.00560 \ \text{Translational Speed*} \\ \text{Translational Speed} \\ + 145.2 \ \text{Plunge Depth*} \\ \text{Plunge Depth} \\ + 1.12 \ \text{Translational Speed*} \\ \text{Plunge Depth} \\ \text{Plunge Depth} \\$$

3.3. Flexural Strength

In accordance with the proposed trend for the tensile strength, in the first stage, the flexural strength results of experiments are presented in order to statistically evaluate the flexural strength results. Table 6 shows the flexural strength results obtained from the experiments.

Table 6
Results of flexural strength experiments.

Run	Translational	Plunge depth	Flexural strength
order	${\rm speed}~({\rm mm/min})$	(mm)	(MPa)
1	45	0.1	96.4
2	75	0.1	72.5
3	45	0.3	72.3
4	75	0.3	62.1
5	60	0.2	76.6
6	60	0.2	77.1
7	60	0.2	76.9
8	30	0.2	70.7
9	90	0.2	63.8
10	60	0	82.3
11	60	0.4	61.9
12	60	0.2	74.1
13	60	0.2	72.3
14	60	0.2	75.5

Similar to the explanations provided in the previous section, the present study uses a complete quadratic model for all models (tensile strength, flexural strength, and hardness). In this model, the main factors, the quadratic power of the main factors, and the interactions of the factors are evaluated. To evaluate the adequacy of the model, graphs of residual normality, constant variances, and time-dependent runs are used. These diagrams have been shown in Fig. 14.

Based on the Percent-Residual and Frequency-Residual diagrams, due to the lack of significant scattering of data (residues) from the normal line and the normal distribution of residual values, it was determined that the data were normally distributed and with these conditions, the data were assumed to be normal, representing a statistically comprehensive representation of the studied models. Also, based on the diagram presented in the Residual-Fitted Value and due to the lack of a special trend in the residuals in relation to the fitted (predicted) values, the accuracy of the assumption that the variances were constant was verified. And according to the Residual-Observation Order diagram and the absence of a specific trend in the residual values with respect to the time and cycle of the simulations, the assumption that the residual values were independent on time was approved. Fig. 13 demonstrates the Pareto chart for the effectiveness of the factors on the flexural strength of the processed specimens. According to the chart presented in Fig. 13, it was found that the most effective parameters on flexural strength were the plunge depth of the tool shoulder and the translational speed, respectively.

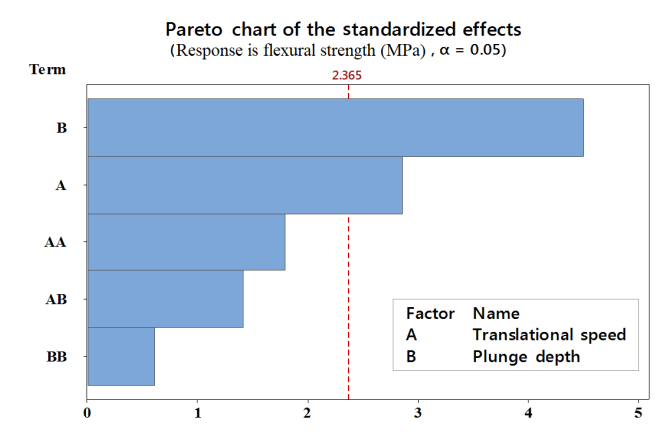


Fig. 13. Pareto chart to determine the order of effect of different factors on flexural strength.

Figs. 15 and 16 investigate the effects of the main parameters on the flexural strength.

Residual Plots for Flexural Strength (MPa)

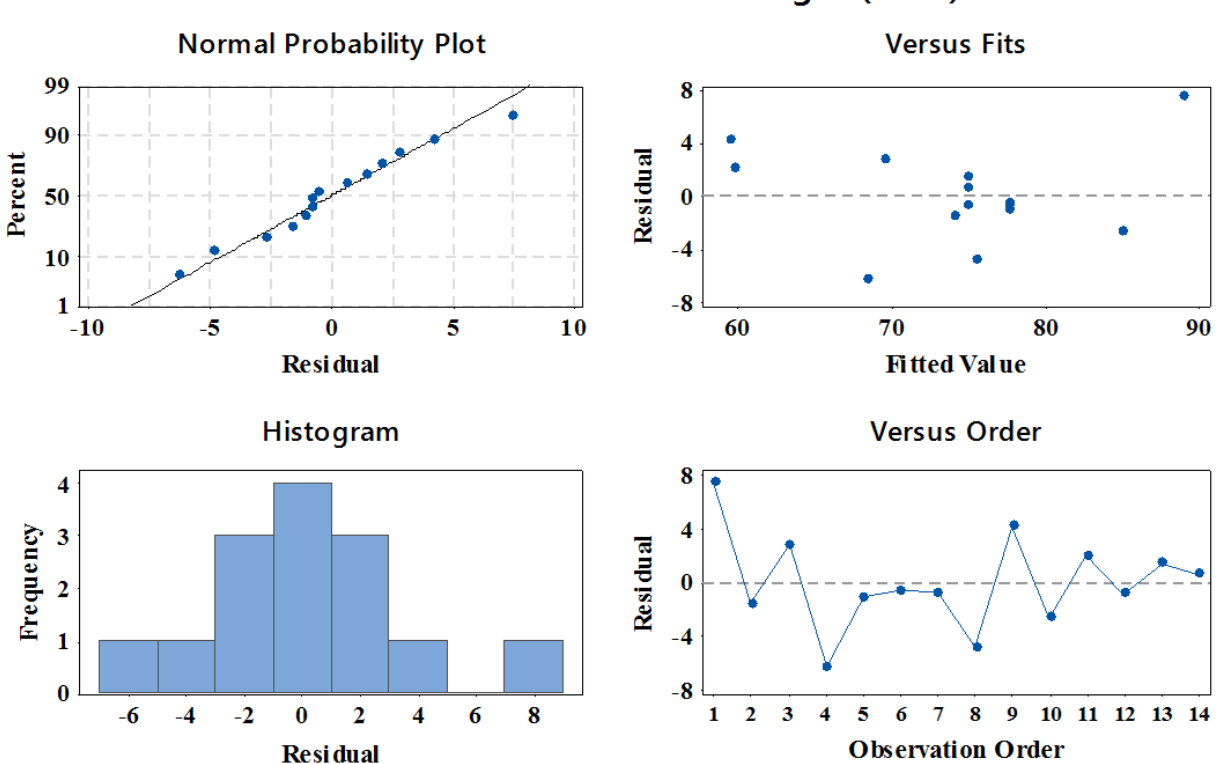


Fig. 14. Diagrams used to evaluate the adequacy of the statistical model of flexural strength.

Main effects plot for flexural strength (MPa)

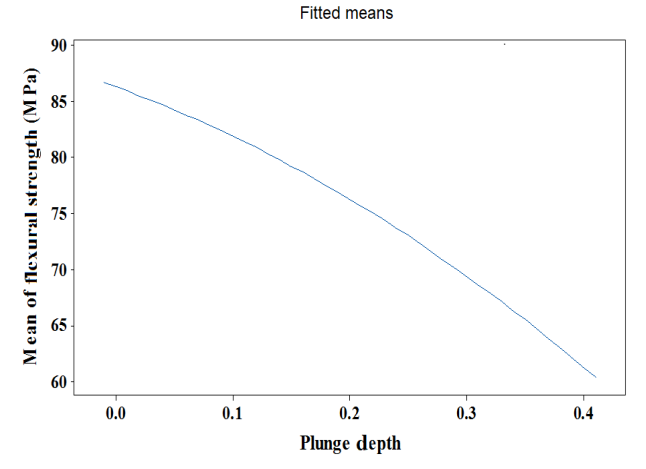


Fig. 15. Diagram of how the plunge depth affects the flexural strength.

Main effects plot for flexural strength (MPa)

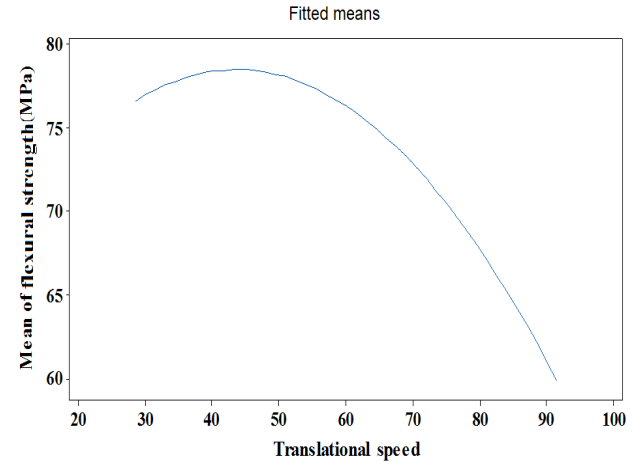


Fig. 16. Diagram of the effectiveness of the translational speed on flexural strength.

Based on Fig. 15, it was found that changes in the plunge depth of the tool's shoulder in the workpiece caused a sharp change in the flexural strength of the processed sample. According to this figure, by increasing the plunge depth of the tool's shoulder in the workpiece, the flexural strength of the processed sample reduced drastically. As observed in Section 3.1.3, increasing the plunge depth leads to the inadequate distribution of Al₂O₃ nano-oxide nanoparticles, and the inhomogeneous distribution and agglomeration of nanomaterials reduces the strength and forms heterogeneity in the mechanical properties of the sample. According to the results, with increasing the plunge depth from 0 to 0.4mm, the flexural strength of the processed sample decreases by 42.6%. According to Fig. 16, it was found that the translational speed had a two-way effect on the flexural strength of the processed specimens: in the first phase, increasing the translational speed from 30 to 46mm/min increased the flexural strength by almost 3%. In the second phase, by increasing the translational speed from 45 to 90mm/min, the flexural strength decreased by 22%. According to the explanations provided, the best translational speed to create the highest flexural strength is between 42 and 46mm/min. In order to statistically predict the value of flexural strength as a function of the studied variables, the flexural strength regression equation was obtained from the statistical software. Eq. (4) shows the regression equation introduced.

Flexural Strength (MPa) = 100.3 + 0.256 Translational Speed -175 Plunge Depth -0.00816 Translational Speed*

Translational Speed -62 Plunge Depth * Plunge Depth +2.28 Translational Speed*

Plunge Depth

3.4. Hardness

Similar to the two parameters of tensile strength and flexural strength, a statistical review of the hardness results is carried out in this section. Table 7 shows the DOE table and the hardness test results of the studied cases.

 Table 7

 Hardness results obtained from the studied samples.

Run	${\it Translational\ speed}$	Plunge depth	${\rm Hardness}$
order	(mm/min)	(mm)	(Vickers)
1	45	0.1	29.5
2	75	0.1	23.2
3	45	0.3	20.1
4	75	0.3	16.8
5	60	0.2	20.2
6	60	0.2	20.4
7	60	0.2	21.1
8	30	0.2	24.2
9	90	0.2	16.7
10	60	0	21.8
11	60	0.4	16.2
12	60	0.2	20.6
13	60	0.2	20.1
14	60	0.2	19.8

For statistical modeling of hardness, a complete quadratic model was used. In this model, the principal factors, the quadratic power of the principal factors, and the interactions of the factors are examined. To evaluate the adequacy of the model, graphs of residual normality, constant variances, and time-dependent runs are used. These diagrams are shown in Fig. 17.

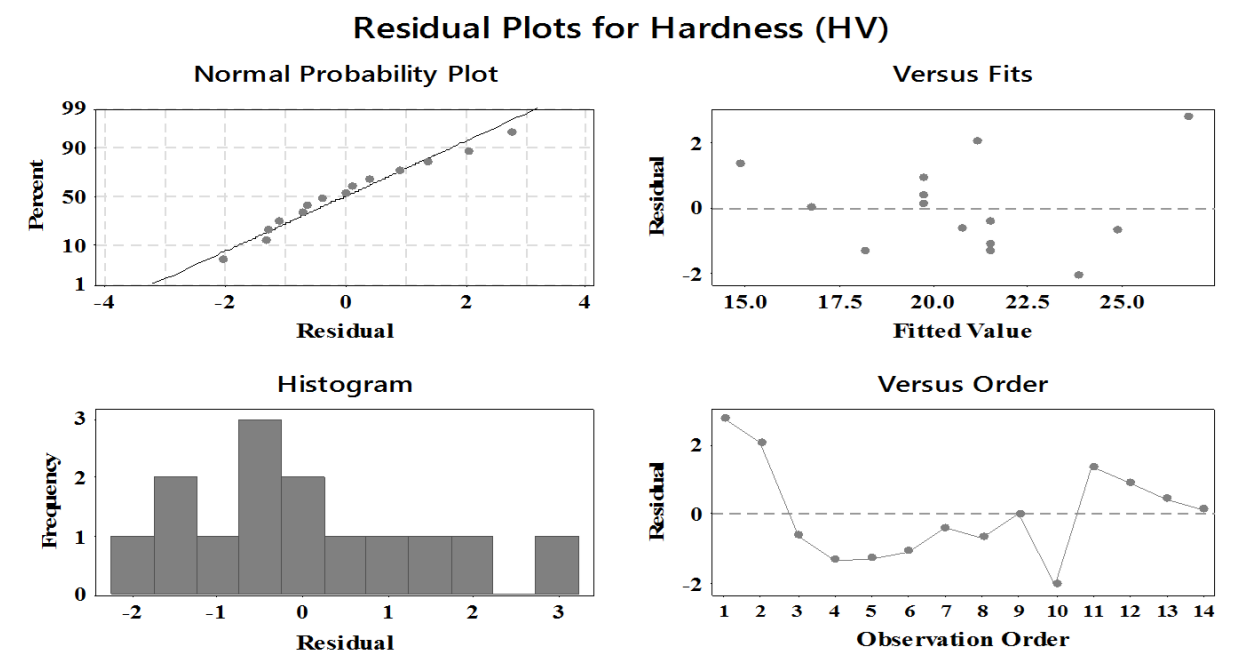


Fig. 17. Diagrams used to evaluate the accuracy of the statistical hardness model.

Based on the Percent-Residual and Frequency-Residual diagrams, due to the lack of significant scattering of data (residues) from the normal line and the relatively normal distribution of residual values, it was determined that the data were normally distributed and with these conditions, the assumption that the data was normal is correct, representing a comprehensive statistically appropriate model for the studied models.

Also, based on the diagram presented in the Residual-Fitted Value and due to the lack of a special trend in the residuals in relation to the fitted (predicted) values, the accuracy of the assumption that the variances are constant is determined. And according to the Residual-Observation Order diagram and the absence of a specific trend in the residual values with respect to the time and cycle of the simulations, the assumption that the residual values are independent on time is approved. Fig. 18 displays the Pareto chart of the effects of the factors on the hardness of processed samples.

According to the Pareto chart presented in Fig. 18, of the main factors, interactions and quadratic power of the main factors, only two main factors directly affect the hardness of the structure. The two factors of plunge depth and translational speed have the greatest effects on the hardness of the processed sample, respectively. Considering the standard effect values of the two factors, it was found that these two factors had almost the same effect on the hardness of the processed sample. Comparing Pareto charts for studying the tensile strength, flexural strength, and hardness, it was found that in all modes, the plunge depth of the tool was the dominant and more effective parameter and changes

in this parameter were effective. In order to investigate the pattern of hardness changes with changes in the two parameters of plunge depth and translational speed, Figs. 19a and 19b illustrate the diagrams of the effects of the main factors on hardness.

According to Figs. 18 and 19, it was found that the trend of hardness changes is the same as changes in plunge depth and translational speed. Based on the obtained results, increasing the translational speed and plunge depth of the tool reduced the hardness of the processed area. By increasing the plunge depth from 0 to 0.4mm and increasing the translational speed from 30 to 90mm/min, the hardness of the processed area decreased by 38.8% and 32.6%, respectively. Eq. (5) presents the regression equation of the statistical software to predict the hardness of the processed area based on the changes of the two factors of plunge depth and translational speed.

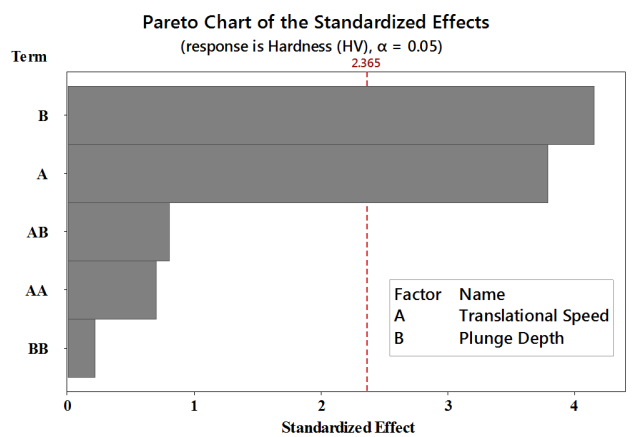


Fig. 18. Pareto chart to determine the order in which different factors affect hardness.

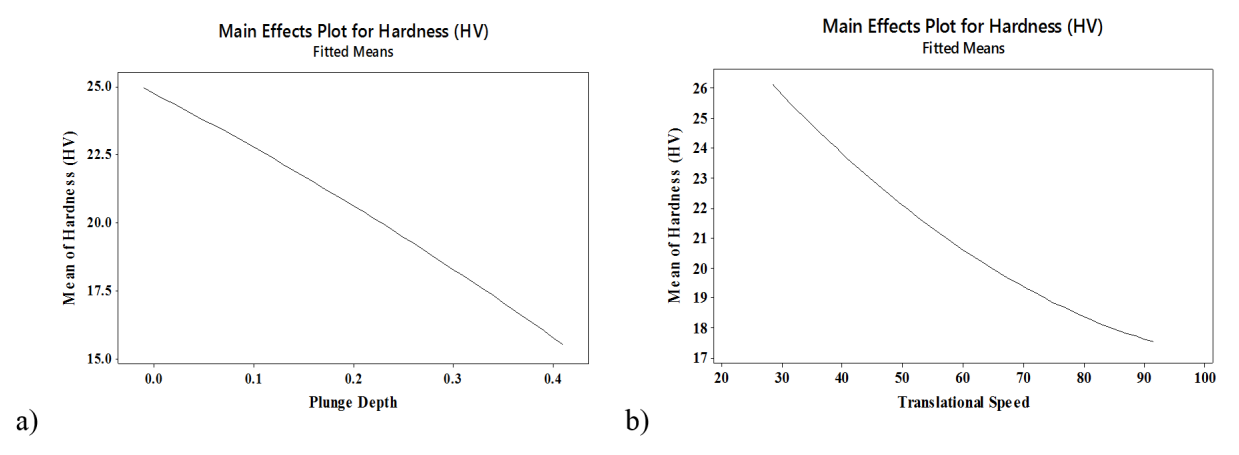


Fig. 19. a) Diagram of how plunge depth affects hardness, b) Diagram of how translational speed is effective on hardness.

 $\begin{aligned} \text{Hardness (HV)} =& 43.4 - 0.384 \text{ Translational Speed} \\ &- 49.0 \text{ Plunge Depth} \\ &+ 0.00123 \text{ Translational Speed*} \\ &- \text{Translational Speed} \\ &- 8.6 \text{ Plunge Depth**} \text{ Plunge Depth} \\ &+ 0.500 \text{ Translational Speed*} \\ &- \text{Plunge Depth} \end{aligned}$

4. Conclusion

The present study investigated the effects of two factors of plunge depth and translational speed on tensile strength, mechanical strength, and hardness of polycarbonate reinforced with ${\rm Al_2O_3}$ nanoparticles. In this section, research results and suggestions for further research in the present field is presented.

- 1) The surface quality of the processed samples was strongly dependent on the two parameters of plunge depth and translational speed. At all translational speeds except 90mm/min, the surface of the processed sample was smooth and free of cavities and protrusions.
- 2) With increasing the plunge depth, the surface quality of the processed area decreased sharply and relatively large protrusions and cavities were formed on the surface of the sample. At two plunge depths of 0 and 0.1mm, the processed surface was relatively smooth and uniform, but at other plunge depths, the quality of the processed surface decreased and relatively large protrusions and cavities were formed in the processed area (turbulence zone).
- 3) It was found that plunge depth had a much stronger effect on the surface quality of the processed samples than the translational speed and

- any change in it caused more drastic changes in the surface quality of the processing area.
- 4) The failure in the base material (pure polycarbonate) was completely smooth and uniform. In other samples, the integrated structure of the processed sample was changed due to the addition of a secondary material (aluminum oxide nanoparticles). In samples with aluminum nanoparticles, the distribution of these nanoparticles determined the type of failure of the loaded sample.
- 5) Increasing the translational speed changed the failure pattern of the samples from ductile failure to brittle failure. With increasing the translational speed from 30 to 60mm/min, the cross-sectional failure occurred almost in a ductile form, but at two translational speeds of 75 and 90mm/min, the failure occurred quite brittle.
- 6) Increasing the plunge depth changed the type of cross-sectional failure from ductile to brittle. Increasing the plunge depth caused severe discontinuities in the welding section.
- 7) Based on the SEM images, it was found that the changes in plunge depth and translational speed led to a significant change in the distribution pattern of nanoparticles in the polymer matrix.
- 8) With increasing the plunge depth in the processed area, the distribution quality of nanoparticles in the polymer matrix decreased sharply. At a plunge depth of 0mm, the nanoparticles were dispersed almost uniformly in the polymer matrix, resulting in a less agglomeration of the nanoparticles. However, in the sample with a larger plunge depth, a relatively severe agglomeration occurred in the processed section.

- 9) At translational speeds of 30 to 60mm/min, the particle distribution in the processed sample was formed almost uniformly.
- 10) It was found that translational speed had a much smaller effect on the distribution pattern of nanoparticles in the polymer matrix than the plunge depth did.
- 11) It was found that the most effective parameters of the model on the values of tensile strength, flexural strength, and hardness of the processed samples were plunge depth and translational speed, respectively. Other terms of the statistical model (interaction factors and quadratic factors) were ineffective.
- 12) Plunge depth was inversely related to the tensile strength of the processed samples. As the plunge depth increased, the tensile strength of the studied samples decreased sharply. According to the statistical analysis, increasing the plunge depth from 0 to 0.4mm reduced the average tensile strength by 52.3%.
- 13) Changing the translational speed caused significant changes in the tensile strength of the processed samples. In the first phase, increasing the translational speed from 30 to 45mm/min caused a relative increase in tensile strength. But then with increasing the speed of 45mm/min, the value of the tensile strength decreased with a significant slope. Averagely, the tensile strength of the processed specimens decreased by 20% by increasing the translational speed from 45 to 90mm/min.
- 14) With increasing the plunge depth, the flexural strength of the processed sample decreased sharply. According to the results, with increasing the plunge depth from 0 to 0.4mm, the flexural strength of the processed sample decreased by 42.6%.
- 15) Evaluating the percentage of reduction in the tensile strength (52.3%) and flexural strength (42.6%) with increasing the plunge depth, it was found that increasing the plunge depth had a more severe effect on the tensile strength and caused a more severe decrease in this parameter.
- 16) Translational speed had a two-way effect on the flexural strength of the processed specimens: in the first phase, increasing the translational speed from 30 to 46mm/min resulted in a flexural strength of approximately 3%. In the second phase, by increasing the translational speed from 45 to 90mm/min, the amount of flexural strength decreased by 22%.

- 17) According to the statistical analysis, the best plunge depth and translational speed to form the highest tensile strength and flexural strength are 0mm and 42-46mm/min, respectively.
- 18) The hardness of the processed sample was inversely proportional to the plunge depth and translational speed. Increasing the plunge depth and translational speed reduced the hardness of the processing area. By increasing the plunge depth from 0 to 0.4mm and increasing the translational speed from 30 to 90mm/min, the hardness of the processed area decreased by 38.8% and 32.6%, respectively.

References

- R.S. Mishra, P.S. De, N. Kumar, Friction Stir Welding and Processing, Science and Engineering, Springer Publisher, (2014).
- [2] Y. Bozkurt, The optimization of friction stir welding process parameters to achieve maximum tensile strength in polyethylene sheets, Mater. Des., 35 (2012) 440-445.
- [3] S. Saeedy, M.B. Givi, Investigation of the effects of critical process parameters of friction stir welding of polyethylene, Proc. Inst. Mech. Eng. Pt. B J. Eng. Manufact., 225(8) (2011) 1305-1310.
- [4] M.A. Rezgui, M. Ayadi, A. Cherouat, K. Hamrouni, A. Zghal, S. Bejaoui, Application of Taguchi Approach to Optimize Friction Stir Welding Parameters of Polyethylene, in EPJ web of conferences. (2010), EDP Sciences.
- [5] A. Arici, S. Selale, Effects of tool tilt angle on tensile strength and fracture locations of friction stir welding of polyethylene, Sci. Technol. Weld. Joining, 12(6) (2007) 536-539.
- [6] A. Arici, T. Sinmazçelýk, Effects of double passes of the tool on friction stir welding of polyethylene, J. Mater. Sci., 40(12) (2005) 3313-3316.
- [7] G. Xie, Z. Ma, L. Geng, Development of a fine-grained microstructure and the properties of a nugget zone in friction stir welded pure copper, Scr. Mater., 57(2) (2007) 73-76.
- [8] H.R. Akramifard, M. Shamanian, M. Sabbaghian, M. Esmailzadeh, Microstructure and mechanical properties of Cu/SiC metal matrix composite fabricated via friction stir processing, Mater. Des., (1980-2015), 54 (2014) 838-844.
- [9] M. Barmouz, M.K.B. Givi, J. Seyfi, On the role of processing parameters in producing Cu/SiC

- metal matrix composites via friction stir processing: Investigating microstructure, microhardness, wear and tensile behavior, Mater. Charact., 62(1) (2011) 108-117.
- [10] R.S. Mishra, Z. Ma, I. Charit, Friction stir processing: a novel technique for fabrication of surface composite, Mater. Sci. Eng., A, 341(1-2) (2003) 307-310.
- [11] A. Shafiei-Zarghani, S. Kashani-Bozorg, A. Zarei-Hanzaki, Microstructures and mechanical properties of Al/Al₂O₃ surface nano-composite layer produced by friction stir processing, Mater. Sci. Eng., A, 500(1-2) (2009) 84-91.
- [12] J. Qu, H. Xu, Z. Feng, D.A. Frederick, L. An, Helge Heinrich, Improving the tribological characteristics of aluminum 6061 alloy by surface compositing with sub-micro-size ceramic particles via friction stir processing, Wear, 271(9-10) (2011) 1940-1945.
- [13] A. Devaraju, A. Kumar, B. Kotiveerachari, Influence of rotational speed and reinforcements on wear and mechanical properties of aluminum hybrid composites via friction stir processing. Mater. Des., 45 (2013) 576-585.

- [14] M. Bahrami, N. Helmi, K. Dehghani, M.K. Be-sharati Givi, Exploring the effects of SiC reinforcement incorporation on mechanical properties of friction stir welded 7075 aluminum alloy: fatigue life, impact energy, tensile strength, Mater. Sci. Eng., A, 595 (2014) 173-178.
- [15] C. Wegst, Key to steel, Stahlschluessel, (1992).
- [16] A. International, ASTM D638-14, Standard Test Method for Tensile Properties of Plastics, (2015) ASTM International.
- [17] A. Norma, E190-92, Standard Test Method for Guided Bend Test for Ductility of Welds, Vol. 03.01. EE. UU.): American Society for Testing and Materials, (2008).
- [18] W.D. Callister Jr, D.G. Rethwisch, Callister's materials science and engineering, John Wiley & Sons, (2020).
- [19] Hardness AB. Standard Test Method for Microindentation Hardness of Materials. ASTM Committee: West Conshohocken, PA, USA. (1999) 384:399.
- [20] T.R. Crompton, Polymer reference book, (2006): iSmithers Rapra Publishing.